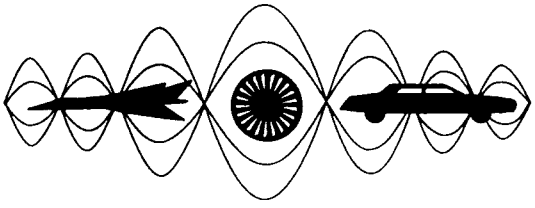

FIFTH INTERNATIONAL CONGRESS ON SOUND AND VIBRATION
DECEMBER 15-18, 1997
ADELAIDE, SOUTH AUSTRALIA

FEM COMPLEX ENVELOPE DISPLACEMENT (CED) ANALYSIS FOR DAMPED HIGH FREQUENCY VIBRATIONS

G. Verbeek, N.C.P.J. Geerts, J.W. Verheij

Faculty of Mechanical Engineering, Eindhoven University of Technology, P.O. Box 513, 5600 MB Eindhoven, The Netherlands, E-mail: bertv@wfw.wtb.tue.nl

Abstract: Complex envelope displacement analysis (CEDA, introduced by Carcaterra and Sestieri) seems to be a promising approach in the mid or high frequency range for vibroacoustic computations. The CED analysis solves for a smooth or low wave number transformed displacement variable from an accordingly transformed partial differential equation, a quasi-static problem. This paper addresses the specific problems that have been solved for generalisation of the original CED analysis to both damped high frequency vibrations in two point boundary value problems as well as the implementation for damped FEM calculations. A numerical example of the longitudinal vibration in a bar is used to illustrate and assess the new FEM method.

1 Introduction

The analysis of linear dynamic (acoustic) systems with deterministic loading, boundary conditions, and material parameters can nowadays be performed by routine Finite/Boundary Element Method (FEM/BEM) calculations. Even for very large systems this approach is feasible by application of commonly used CMS reduction techniques. However the FEM analysis, or any other discretisation technique, still is limited to a frequency band with a sufficiently low upper excitation frequency, according to the Shannon sampling theorem. An explicit low frequency range restriction will be present in future deterministic FEM models, despite of the increasing computer power.

On the other hand, for engineering applications, Statistical Energy Analysis (SEA) provides good average results for ensembles of structures in the high frequency range (Lyon and DeJong, 1995). But the application of the SEA is restricted to a frequency band above an explicit high frequency limit, dictated by the assumptions of SEA like a high enough modal density. Other deficiencies are the lack of information on the distribution of the results and the need for a very experienced analyst for modelling the SEA subsystems.

Up till now no alternative engineering tools are available for SEA in the high frequency range, or even any tools for the mid frequency range. So the volume of research on these subjects is increasing, especially during the last decade. For a brief review, see e.g. Carcaterra and Sestieri (1997).

A literature search on alternative methods to SEA (Raaymakers, 1995), showed three main research topics: Thermal Analogons (e.g. Nefske and Sung, 1987; Cho and Bernhard, 1993), which are proved to be exact only for 1-D systems (Carcaterra and Sestieri, 1995a; Xing and Price, 1997); FRF methods (Girard and Defosse, 1993), which rely on smoothed FRFs that are not analytically available for general structures; and Envelope methods (Carcaterra and Sestieri, 1995b,c, 1997; Sestieri and Carcaterra, 1996) of which the Complex Envelope Displacement Analysis (CEDA) is the most general and promising approach. No approximations are made so that the CEDA linear operator transformed quasi-static differential equation is completely equivalent to the original physical differential equation, in contrast with the other methods.

Towards the application of CED analysis as an engineering tool, several drawbacks of the original CED analysis must be solved:

- the occurrence of spurious high wave number solutions;
- application of FEM (or another discretisation technique) to the damped CED analysis;
- the problems with the unknown CEDA boundary conditions;
- application to higher order and more dimensional systems;
- extension to statistical systems, as to-date, the method is limited to deterministic problems.

This paper deals with the first three items of the above list. The fourth subject is not a fundamental problem for 1-D systems, for higher dimensions it is studied by Sestieri and co-workers. The final subject is studied at present.

So, in this presentation, the generalisation of the original CED analysis to damped high frequency vibrations in two point boundary value problems is dealt with. The Finite Element Method will be used which automatically eliminates the spurious solution problem, and a method for correct inclusion of the CEDA boundary conditions is presented. Finally a numerical example of the longitudinal vibrations in a bar is used to illustrate and assess the new FEM method.

2 Undamped CED Analysis

The idea behind CEDA is a signal transformation which transforms a real high frequency signal and differential equation into a complex low frequency signal and corresponding differential equation, respectively. An outline of the theory is presented here, for a more detailed presentation is referred to Carcaterra and Sestieri (1997).

2.1 Theory

The signal transformation consists of three steps. The first is the computation of the Hilbert transform $\tilde{u}(x)$ of the displacement field or signal $u(x)$, which is defined as the convolution of $u(x)$ with $1/\pi x$:

$$\tilde{u}(x) = \frac{1}{\pi x} * u(x) = \int_{\xi=-\infty}^{\infty} \frac{1}{\pi x} u(x-\xi) d\xi. \tag{1}$$

Subsequently the analytic signal $\hat{u}(x)$ can be defined as:

$$\hat{u}(x) = u(x) + j\tilde{u}(x), \tag{2}$$

which possesses the useful property that it only has a positive wave number contents. In the third step, the Complex Envelope $\overleftarrow{u}$ is now defined by multiplying the analytic signal $\hat{u}$ by $e^{-jk_s x}$:

$$\overleftarrow{u}(x) = \hat{u}(x) e^{-jk_s x}, \tag{3}$$

in which k_s is the shifting wave number. Under the assumption of a band limited wave number contents of the physical displacement, this new smooth CEDA variable will be wave number band limited at a much lower wave number, so it can be sampled at a much lower rate. Now this complex envelope displacement should be computed from an CEDA transformed differential equation.

As an example in this paper the equation of motion for undamped harmonic longitudinal vibration in a clamped-clamped bar of unit length is discussed:

$$-\omega^2 \rho A u(x) - EA u''(x) = p(x) \quad ; \quad u(0) = u(1) = 0. \tag{4}$$

Where $u''(x)$ is the second derivative of the longitudinal displacement $u(x)$, $p(x)$ is the body force amplitude per unit length, and ω stands for the excitation frequency.

Since the Hilbert transform is a linear transformation, equation (4) is valid for the Hilbert transforms of $u(x)$ and $p(x)$, as well as their analytic signals:

$$-\omega^2 \rho A \hat{u}(x) - EA \hat{u}''(x) = \hat{p}(x). \tag{5}$$

With the relation for the complex envelope and the analytic signal, equation (3), written inversely:

$$\hat{u}(x) = \overleftarrow{u}(x) e^{+jk_s x}, \tag{6}$$

we can write for the second derivative of the analytic signal $\hat{u}(x)$:

$$\hat{u}''(x) = [\overleftarrow{u}''(x) + 2jk_s \overleftarrow{u}'(x) - k_s^2 \overleftarrow{u}(x)] e^{jk_s x}. \tag{7}$$

The differential equation can now be written as (the term $e^{jk_s x}$ is factored out):

$$-\omega^2 \rho A \overleftarrow{u}(x) - EA[\overleftarrow{u}''(x) + 2jk_s \overleftarrow{u}'(x) - k_s^2 \overleftarrow{u}(x)] = \overleftarrow{p}(x). \tag{8}$$

It can simply be seen that, if the shifting wave number k_s is chosen equal to the excitation wave number $k = \omega/\sqrt{E/\rho}$, the zero order terms cancel out another. If k_s is close to

the wave number k, the mass contribution to the equations is small and therefore the transformed differential equations can be called quasi-static.

The real physical signal can be reconstructed without loss of information by the simple inverse transformation on the complex envelope signal $\overleftarrow{u}(x)$:

$$u(x) = \mathrm{Re}\left\{\overleftarrow{u}(x)^{+jk_s x}\right\}. \tag{9}$$

The multiplication with $e^{jk_s x}$ increases the frequency of $u(x)$ and therefore $u(x)$ will have higher frequency contents than $\overleftarrow{u}(x)$. When working with discrete signals it is therefore necessary to resample $\overleftarrow{u}(x)$with an interpolation routine.

2.2 FEM discretisation

For clarity, in this specific discretisation a standard Galerkin weighted residual approach with linear elements is used. This is not a restriction to the CED analysis, as for the actual computations both linear and quadratic elements have been used.

The weighted residual formulation of the CEDA problem (8) is:

$$\int_0^L \eta(x)\{-\omega^2\rho A\overleftarrow{u} - EA[\overleftarrow{u}'' + 2jk_s\overleftarrow{u}' - k_s^2\overleftarrow{u}\}\,dx = \int_0^L \eta(x)\overleftarrow{p}(x)\,dx. \tag{10}$$

By using the Galerkin approach, both $u_e(x)$ and the test functions $\eta_e(x)$ will be discretised per element with linear interpolation functions:

$$\overleftarrow{u}_e(x) = \eta_e(x) = \mathbf{N}_e(x)\overleftarrow{\mathbf{u}}_e = \left[\tfrac{1}{2}(1-\xi) \quad \tfrac{1}{2}(1+\xi)\right]\begin{pmatrix}\overleftarrow{u}_1\\ \overleftarrow{u}_2\end{pmatrix}_e \quad ; \quad -1 < \xi < 1. \tag{11}$$

Elaboration, for one element, of the first term in the left hand side of equation (10) gives the classical mass matrix:

$$\int_0^{L_e} \eta(x)\rho A\overleftarrow{u}(x)\,dx \quad \Longrightarrow \quad \mathbf{M}_e = \frac{\rho A L_e}{6}\begin{bmatrix}2 & 1\\ 1 & 2\end{bmatrix}. \tag{12}$$

Integration by parts of the second term of the weak formulation (10) gives:

$$\int_0^{L_e} -\eta(x)EA\overleftarrow{u}''\,dx = \int_0^{L_e} \eta' EA\overleftarrow{u}'\,dx - \left[\eta EA\overleftarrow{u}'\right]_0^{L_e}. \tag{13}$$

The first term on the right hand side of this equation results in the standard stiffness matrix:

$$\int_0^{L_e} \eta' EA\overleftarrow{u}'\,dx \quad \Longrightarrow \quad \mathbf{K}_e = \frac{EA}{L_e}\begin{bmatrix}1 & -1\\ -1 & 1\end{bmatrix}. \tag{14}$$

In classical FEM the boundary term in the right hand side of equation (13) can be moved to the right hand side of the resulting set of algebraic equations and describes the external forces on the boundary nodes. In CEDA-FEM a correction has to be made since the constitutive relation also undergoes a transformation (see equations (4)–(8)):

$$F = EAu' \quad \Longrightarrow \quad \overleftarrow{F} = EA[\overleftarrow{u}' + jk_s\overleftarrow{u}]. \tag{15}$$

and therefore the boundary term transforms into:

$$-\left[\eta EA\overleftarrow{u}'\right]_0^{L_e} = \left[j\eta EAk_s\overleftarrow{u}\right]_0^{L_e} - \left[\eta\overleftarrow{F}\right]_0^{L_e}. \tag{16}$$

As will be explained in the next subsection, the boundary forces are negligible, so the second term can be put equal to zero and the first boundary term gives rise to an extra matrix:

$$\left[j\eta EAk_s\overleftarrow{u}\right]_0^{L_e} \quad \Longrightarrow \quad \mathbf{C}_{eB} = jk_sEA\begin{bmatrix}-1 & 0\\ 0 & 1\end{bmatrix}. \tag{17}$$

More attention is paid to the non classical third and fourth terms that are introduced in the CEDA weighted residual formulation equation (10). The real term gives a symmetric matrix that is proportional to the mass matrix, and the imaginary term leads to an skew-symmetric matrix:

$$\int_0^{L_e}\eta(x)EA[-k_s^2\overleftarrow{u}+j2k_s\overleftarrow{u}']\,dx \quad \Longrightarrow$$

$$\mathbf{C}_{eR} = \frac{EAk_s^2L_e}{6}\begin{bmatrix}2 & 1\\ 1 & 2\end{bmatrix} \quad ; \quad \mathbf{C}_{eI} = jk_sEA\begin{bmatrix}1 & -1\\ 1 & -1\end{bmatrix}. \tag{18}$$

The full complex algebraic set of equations for a single CEDA element are:

$$\left[-\omega^2\mathbf{M}_e + \mathbf{K}_e + \mathbf{C}_{eR} + j\left(\mathbf{C}_{eI}+\mathbf{C}_{eB}\right)\right]\overleftarrow{\mathbf{u}}_e = \int_0^{L_e}\mathbf{N}_e^T(x)\overleftarrow{p}(x)\,dx. \tag{19}$$

It can be observed that $\mathbf{C}_{eR}$ can cancel out $-\omega^2\mathbf{M}_e$ if k_s is chosen equal to k, and again, the problem is reduced from a high frequency dynamic problem to a static problem.

Standard assembling of all element matrices leads to a set of N complex algebraic equations for the complete system. For application of the boundary conditions, this system will be split up in real and imaginary parts to form a set of $2N$ real equations.

2.3 Boundary conditions

The boundary conditions, in this case prescribed displacements and unknown clamping forces, are dealt with in a non-standard way.

The physical second order differential equation (4) needs two boundary conditions, in this case prescribed displacements:

$$u(0) = u_0 \quad ; \quad u(1) = u_1. \tag{20}$$

In CEDA notation boundary conditions on the complex envelope variable are needed. The relation to the boundary conditions of the original problem is given by the back transformation (9) and can be split up in real $(\overleftarrow{u}_r(0), \overleftarrow{u}_r(1))$ and imaginary parts $(\overleftarrow{u}_i(0), \overleftarrow{u}_i(1))$:

$$\begin{cases}\mathrm{Re}\left\{\overleftarrow{u}e^{jk_sx}\right\}_{x=0} & = u_0\\ \mathrm{Re}\left\{\overleftarrow{u}e^{jk_sx}\right\}_{x=1} & = u_1\end{cases} \quad \Longrightarrow \quad \begin{cases}\left[\cos(k_sx)\overleftarrow{u}_r - \sin(k_sx)\overleftarrow{u}_i\right]_{x=0} & = u_0\\ \left[\cos(k_sx)\overleftarrow{u}_r - \sin(k_sx)\overleftarrow{u}_i\right]_{x=1} & = u_1\end{cases}. \tag{21}$$

Now two real unknowns in the set of $2N$ algebraic equations can be eliminated, resulting in a $2N \times (2N-2)$ system matrix.

In classical FEM the system could be solved for the $2N-2$ unknowns by partitioning to a $(2N-2) \times (2N-2)$ system, after which the 2 unknown boundary forces could be computed by postprocessing. However, in CED analysis this can not be done because the physical delta distribution boundary forces $(F(0), F(1))$ will lead to a CEDA force field, theoretically, over an infinite domain. But, the CEDA distribution can be split up in the unknown physical amplitudes $F_{0,1}$ and their corresponding analytically known functions $\overleftarrow{\delta}_{0,1}$, e.g. for $x = 1$:

$$F(1) = F_1\,\delta(x-1) \quad \Longrightarrow \quad \overleftarrow{p}(1) = F_1\,\overleftarrow{\delta}_1(x-1) = F_1\left(\delta(x-1) + j\frac{1}{\pi(x-1)}\right)e^{-jk_s x}. \tag{22}$$

This has two important consequences. First, the discretised domain has to be extended beyond the clamping points of the bar to a point where the clamping force distribution is negligible (this is the reason why the point CEDA boundary forces in the discretisation process could be eliminated). Second, the physical boundary forces have to be kept in the solution process. The CEDA distributed load contribution to the discretised system, the right hand side of equation (19), can now for the complete system be written as:

$$\begin{aligned}\int_0^L \mathbf{N}^T(x)\overleftarrow{p}(x)\,dx &= \int_0^L \mathbf{N}^T(x)\{\overleftarrow{p}_{exc}(x) + \overleftarrow{p}_0(x) + \overleftarrow{p}_1(x)\}\,dx = \\ \int_0^L \mathbf{N}^T(x)\overleftarrow{p}_{exc}(x)\,dx &+ F_0\int_0^L \mathbf{N}^T(x)\overleftarrow{\delta}_0(x)\,dx + F_1\int_0^L \mathbf{N}^T(x)\overleftarrow{\delta}_1(x)\,dx = \\ &\int_0^L \mathbf{N}^T(x)\overleftarrow{p}_{exc}(x)\,dx + F_0\,\boldsymbol{\delta}_0 + F_1\,\boldsymbol{\delta}_1. \end{aligned} \tag{23}$$

Rearranging all unknowns to the left hand side of the system of equations, finally results in a square $2N \times 2N$ uniquely solvable real system of equations, for $2N-2$ real/imaginary components of the N nodal CEDA variables, and 2 physical boundary forces. The remaining 2 real/imaginary components of the nodal CEDA variables can be computed by using the boundary conditions (21).

3 Damped CED Analysis

As already stated in Carcaterra and Sestieri (1997) the introduction of damping in CEDA differential equations is not trivial. The solution to a damped problem is a complex displacement, and because the CEDA transform is only applicable to real signals the complex displacement and the corresponding differential equation must be split up in real and imaginary components. After that, the real and imaginary parts of the physical variable can be both CEDA transformed to two complex envelope displacement variables.

Starting from the damped variant of differential equation (4):

$$-\omega^2\rho A u(x) + j\omega c_d u - EAu''(x) = p(x) \quad ; \quad u(0) = u(1) = 0, \tag{24}$$

we can split up: the solution $\mathbf{u} = (u_r\ u_i)^T$, the excitation distribution $\mathbf{p} = (p_r\ p_i)^T$, and the differential equation in real and imaginary components:

$$-\omega^2 \rho A\, \mathbf{I}\, \mathbf{u}(x) + j\omega c_d \begin{bmatrix} 0 & -1 \\ 1 & 0 \end{bmatrix} \mathbf{u}(x) - EA\, \mathbf{I}\, \mathbf{u}''(x) = \mathbf{p}(x). \tag{25}$$

Now the CEDA transform can be performed, which gives:

$$\left[-\omega^2 \rho A\, \mathbf{I} + j\omega c_d \begin{bmatrix} 0 & -1 \\ 1 & 0 \end{bmatrix} \right] \overleftarrow{\mathbf{u}}(x) - EA\, \mathbf{I} \left(\overleftarrow{\mathbf{u}}''(x) + 2jk_s \overleftarrow{\mathbf{u}}'(x) - k_s^2 \overleftarrow{\mathbf{u}}(x) \right) = \overleftarrow{\mathbf{p}}(x). \tag{26}$$

Following the recipe of the previous section there will be no fundamental difficulties in discretising this set of CEDA differential equations. This work has been carried out and the results are programmed in MATLAB for linear and quadratic elements.

4 Numerical example

A longitudinal vibrating clamped-clamped bar with length $L = 1$ [m], density $\rho = 7800$ [kg/m^3], Young's modulus $E = 210\ 10^9$ [N/m^2], damping $c_d = 7020$ [Ns/m^2] (loss factor $\eta = c_d/(\rho\omega A) = 0.03$ [$-$]) and area $A = 1\ 10^{-4}$ [m^2] is excited at $x = 0.4$ [m] with an harmonic oscillating force with amplitude $F_0 = 1000$ [N] and angular frequency $\omega = 3\ 10^5$ [rad/s]. The expected number of waves per meter is $1/\lambda = k/(2\pi) = 9.2$.

To obtain a reference solution, a classical damped FEM analysis with 100 quadratic elements has been performed. In the sequel this is called the exact solution. From the complex response, the real and absolute values are plotted in figure 1. Note the decaying solution due to damping.

If we look at the Fourier transform of the real part of the complex solution, see figure 2, we see that an important assumption of CED analysis is not met. The solution is not really band limited, the spatial frequency $(k/(2\pi))$ is significant in the range of 0 up to 20–25 waves per meter.

In figure 3 the CEDA transform of the real part of the exact solution is plotted, as well as the corresponding Fourier transform. One can observe that the CEDA variable seems to be reasonably smooth, but the discontinuity, at the excitation point $x = 0.4$, and small oscillations in the excitation wave number are still present. So, the wave number range is only reduced by a factor of two, up to approximately 10 waves per meter. Therefore, in this example, a CEDA-FEM solution should contain at least 20 quadratic elements plus some extra elements outside the classic interval (see subsection 2.3).

The results of the damped CEDA-FEM calculation with $4 + 20 + 4$ elements, as well as the exact solution, are plotted in figure 1. The response is computed correctly with an error of approximately 10 percent, which would have been the same if we would have used 50 classical elements. A more accurate CEDA-FEM computation with $10 + 50 + 10$ elements results in the exact solution. Discretisation with fewer than $4 + 20 + 4$ elements, as with classical FEM, results of course in an erroneous under sampled solution.

5 Conclusions

A new damped CEDA-FEM method has been derived successfully. No spurious solutions as reported by Carcaterra were found, and the addition of damping did not lead to

fundamental problems. A non standard inclusion of the CEDA boundary conditions for displacements, as well as the boundary forces was presented.

It is shown that the expected large reduction in the number of elements for computing the CEDA response has not been accomplished. The spatial point excitation in this example, and the examples in Carcaterra's articles, does not result in a wave number band limited response, one of the basic assumptions of the CED analysis. The main reduction in the number of elements for these type of signals is only a factor of two. The total reduction in this example is therefore limited to somewhat less than a factor of two, due to the small number of extra elements that are needed outside the original domain, for correct inclusion of the boundary conditions.

References

Carcaterra, A. and Sestieri, A. (1995a). Energy density equations and power flow in structures. *Journal of Sound and Vibration*, **188**(2), 269–282.

Carcaterra, A. and Sestieri, A. (1995b). An envelope energy model for high frequency dynamic structures. *Journal of Sound and Vibration*, **188**(2), 283–295.

Carcaterra, A. and Sestieri, A. (1995c). Envelope versus envelope-phase model for high frequency structural problems. In *IMAC 13*, Nashville, USA.

Carcaterra, A. and Sestieri, A. (1997). Complex envelope displacement analysis: A quasi-static approach to vibrations. *Journal of Sound and Vibration*, **201**(2), 205–233.

Cho, P. E. and Bernhard, R. J. (1993). A simple method for predicting energy flow distributions in frame structures. In *4th International Congress on Intensity Techniques*, pages 347–354, Senlis, France. CETIM.

Girard, A. and Defosse, H. (1993). Frequency response smoothing, matrix assembly and structural paths: a new approach for structural dynamics up to high frequencies. *Journal of Sound and Vibration*, **137**(1), 53–68.

Lyon, R. H. and DeJong, R. G. (1995). *Theory and application of statistical energy analysis*. Butterworth-Heineman, second edition.

Nefske, D. J. and Sung, S. H. (1987). Power flow finite element analysis of dynamic systems: Basic theory and application to beams. In *ASME Publication NCA-3: Statistical Energy Analysis*, pages 47–54.

Raaymakers, J. A. L. J. (1995). Alternative methods to SEA in mid and high frequency dynamics. WFW-report 95.161, Eindhoven University of Technology, The Netherlands. In Dutch.

Sestieri, A. and Carcaterra, A. (1996). Circumventing space sampling limitations in mechanical vibrations. *Meccanica*, **31**, 163–176.

Xing, J. T. and Price, W. G. (1997). The energy flow equation of continuum dynamics. In *IUTAM Symposium on: Statistical Energy Analysis*, Southampton, UK.

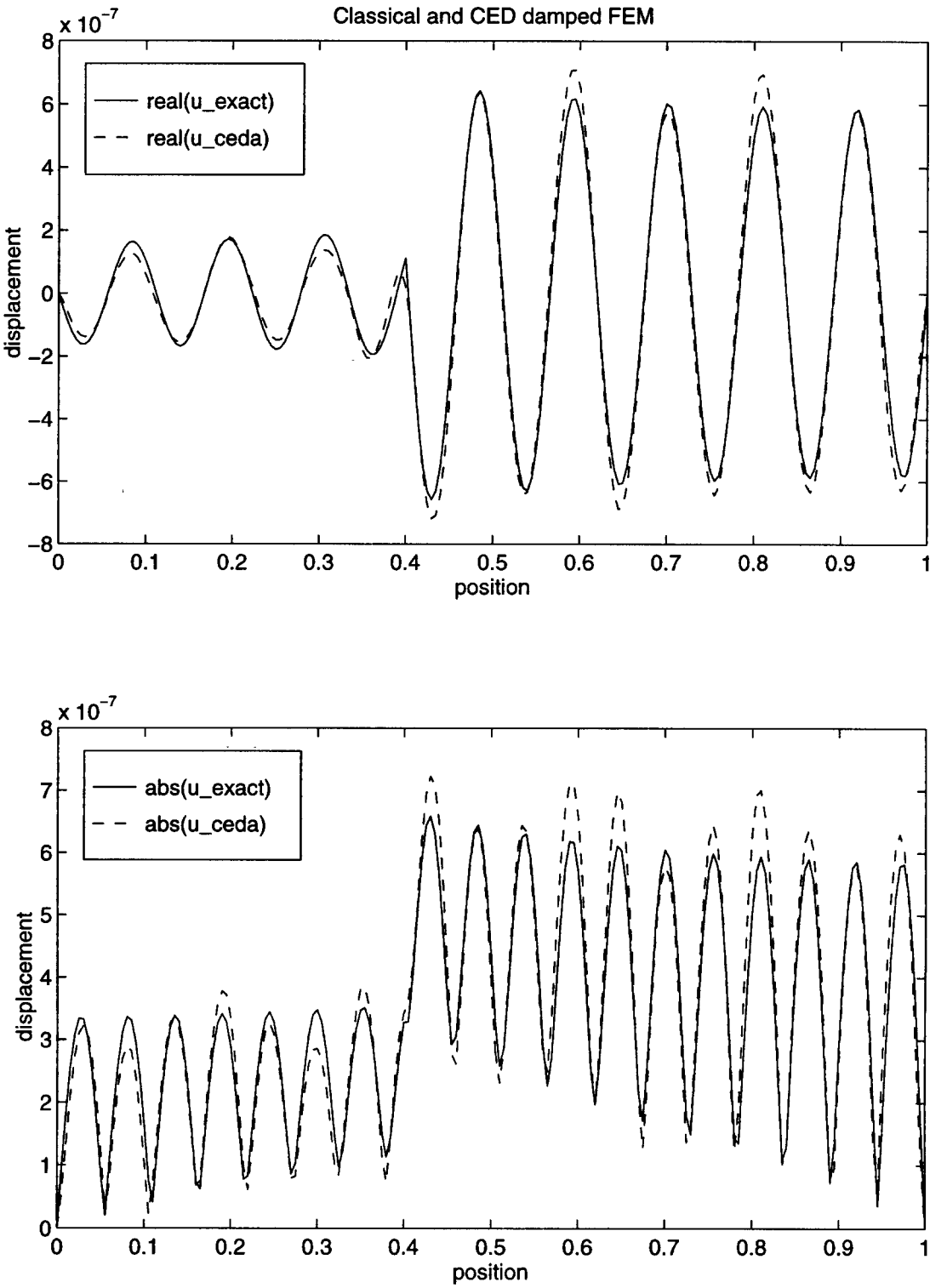

Figure 1: The complex physical displacement results of classical damped FEM versus damped CEDA-FEM. In the upper graph the real part of the complex longitudinal displacement is plotted. In the lower graph the corresponding absolute value is drawn.

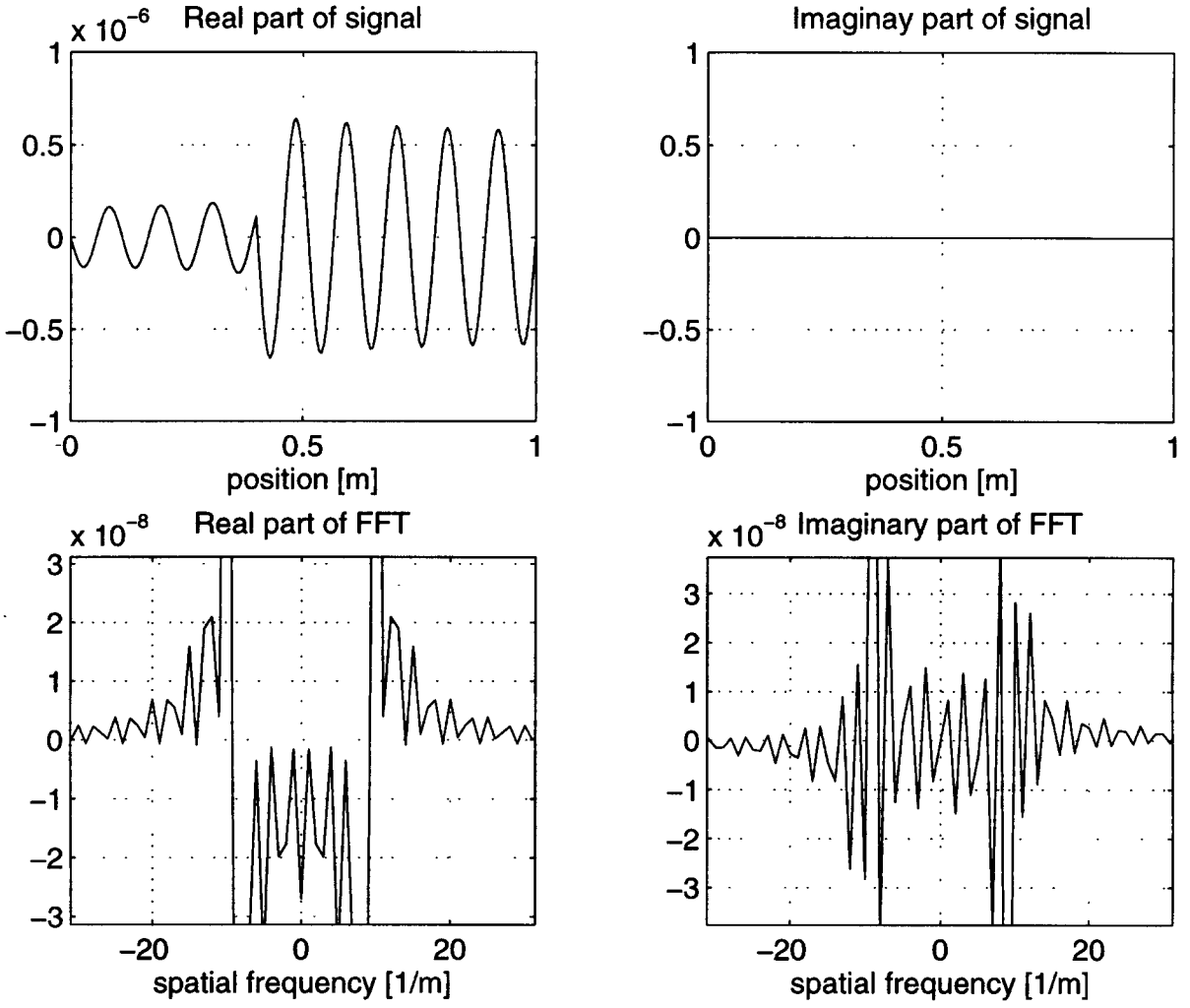

Figure 2: The Fourier transform of the real part of the exact physical displacement (zoomed in to $-30, 30$ [1/m]).

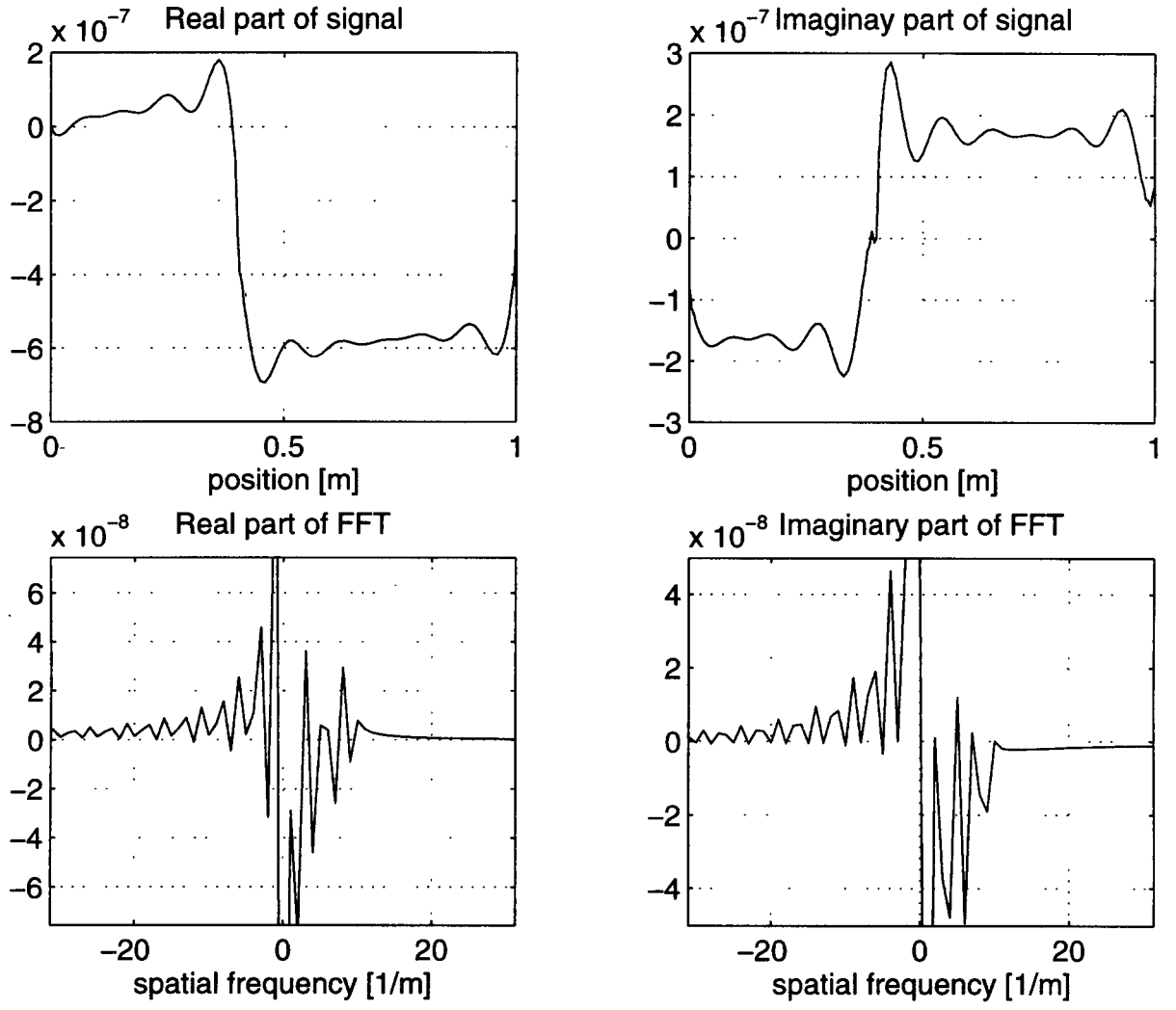

Figure 3: The CEDA transform and its Fourier transform of the real part of the exact physical displacement (zoomed in to $-30, 30$ [1/m]).